On the Applicability of Deterministic Modelling to Indoor UWB Channels

J.JEMAI[1], P. EGGERS[2], G.F. PEDERSEN[2], T.KÜRNER[1]
[1]IfN, Braunschweig Technical University, e-mail: Jemai, Kuerner@ifn.ing.tu-bs.de
[2] CPK, Center for PersonKommunikation, Aalborg University, email: pe, gfp@cpk.auc.dk

Abstract - This paper reports on the results of Ultra-Wideband measurements for several scenarios from 2 GHz to 6 GHz within an office building and investigates the applicability of deterministic modelling through 3D ray tracing to UWB channels. The blind prediction, based on the a priori knowledge of material parameters and on measured antenna radiation patterns, uses a sub-band-divided ray tracing. Measured time dispersion channel parameters such as channel impulse response in time domain and transfer function in frequency domain, delay spread, power delay profile and impulse response, have been compared with blind deterministic prediction. Moreover large-scale parameters including total path loss and frequency decaying factor have been computed for both measurements and the prediction model.

1 Objective and Introduction

Basic indoor positioning systems for instance with WiFi use a database containing the signal strength footprints. Moreover, by the deployment of UWB systems the resolvability of the different multipath components has been an easier way to enable the extraction of the time of arrival. These positioning techniques usually need an extensive footprint database either of signal strength or channel impulse response [1]. Thus, channel modelling and radio coverage prediction is a solution to get a quick and cheaper alternative to the measurement campaigns. The UWB signal strength and impulse response prediction would therefore be of great interest.

The UWB channel can be characterised mainly by two features which are spatial resolution and frequency behaviour. Thus, due to the higher bandwidth, a small time delay resolution can be reached and therefore certain propagation paths can be distinguished from each other. UWB signals also enable fine space resolution. Currently, UWB communication is being investigated by several research groups to provide some understanding of the UWB channel behaviour. An overview of these investigations is presented in [2]. Moreover, UWB channels are characterised by a frequency selective fading pattern. Apart from the frequency dependent variation of the antenna radiation pattern, electromagnetic material parameters show frequency selective behaviour. Propagation mechanisms like reflection, transmission and diffraction depend on the variation of the electromagnetic material parameters with frequency. In general, a power decay with increasing frequency can be assessed, the main part of power is localised towards the lower frequencies [3]. Since UWB signals do not fulfill narrowband assumptions, a modified version of the deterministic modelling with ray tracing will be presented.

The main goal of this paper is the evaluation of the applicability of a deterministic modelling through 3D ray tracing to UWB channels. It is examined and discussed through measurement examples whether the deterministic modelling could be applied to predict UWB channel properties and behaviour,. This paper is organised as follows: Section 2 focuses on the deterministic modelling of the indoor UWB channel through ray tracing prediction using sub-bands combining technique. Section 3 deals with the measurements performed in office environment for LOS intra-office, NLOS corridor-office and measurements on corridor. The applicability of the deterministic modelling for UWB channels will be examined and discussed in Section 4.

2 Blind Prediction Model: Band-Divided Ray Tracing

A simulation tool based on a 3D ray tracing technique has been developed in order to predict the indoor radio propagation including the impulse response as well as the fieldstrength at any transmitter and receiver position. This model requires an accurate 3D indoor database with detailed information describing the walls, their thickness, the used building materials and their dielectric properties as well as the positions of doors and windows. The required building parameters introduced in the database are the relative permittivity and the tangent loss which are related to the reflection and transmission factors respectively. Besides the free space propagation, this tool considers multiple reflections, diffraction according to the Uniform Theory of Diffraction (UTD) as well as transmission through walls. The resulting CIR is derived taking into account azimuth and elevation of both transmitter and receiver as well as the AoD and AoA of propagation paths. As ray tracing modelling does not consider wideband assumptions, the prediction model has to be adapted. Therefore a band-divided ray tracing method has been used. This method has been earlier introduced in [4]. The frequency bandwidth of 4 GHz has been divided into 8 sub-bands with 500 MHz each. In this work, the simplifying assumption that material parameters and antenna radiation patterns are invariant and non-frequency selective over a bandwidth of 500 MHz has been made. Therefore, the combination of simple narrowband prediction in order to characterise the ultra-wideband channel will be assessed. A deterministic ray tracing model has been used to determine a delay profile at the central frequency of each sub-band. Electromagnetic material parameters for the different sub-bands have been introduced into the building database so that a blind prediction can be assessed. The electromagnetic material parameters related to the permittivity (ε_r) and the tangent loss ($tg\delta$) used in the building database are taken from measurements from earlier publications [5][6][7] and are shown in Figure 1a and 1b.

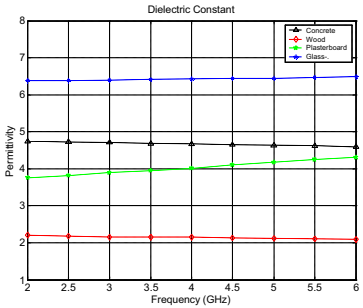

Figure 1a. Relative permittivity of considered building materials

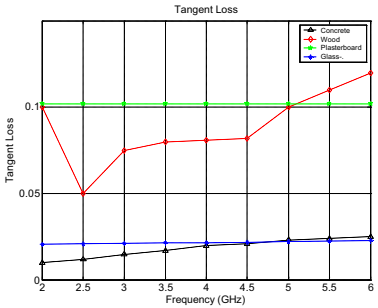

Figure 1b. Tangent loss of considered building materials

The delay profiles (Figure 2b) are Fourier-transformed into frequency responses around each sub-band central frequency. The parts around the sub-band frequency have been extracted from the frequency response. Hence, the different parts at different frequencies are extracted and combined (Figure 2a).

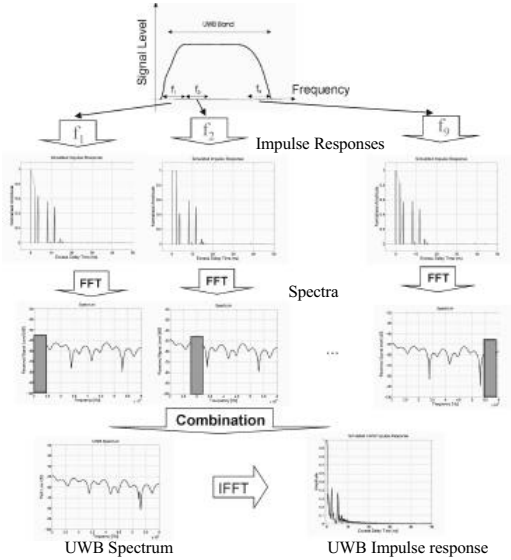

Figure 2a. Sub-band divided ray tracing

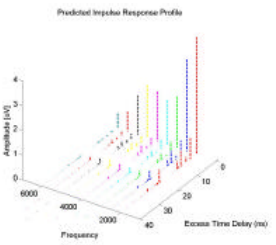

Figure 2b. Sub-band divided ray tracing

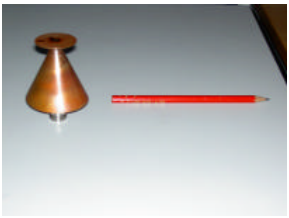

Figure2c. UWB-Discone Antenna

Figure 3 shows the omnidirectional discone antenna used for the measurements. Moreover, the used radiation patterns were measured in 3D within an anechoic chamber at each sub-band of 500 MHz bandwidth from 2 GHz to 6 GHz. Figure 3a and 3b show the measured horizontal and vertical power radiation gain patterns of the used omnidirectional discone antenna.

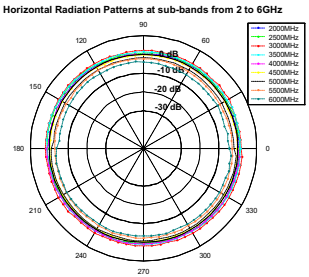

Figure 3a. Horizontal radiation patterns of the discone antenna at sub-bands

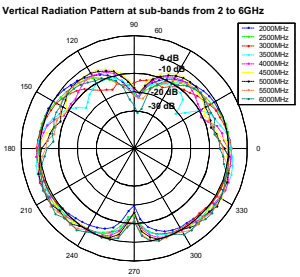

Figure 3b. Vertical radiation patterns of the discone antenna at sub-bands

In this work, only scattering from interacting objects the size of which is much greater compared to the biggest wavelength (15 cm) within the UWB signal has been considered. The deterministic model based on blind 3D ray tracing predictions has been applied to the same configurations where the measurements have been conducted. The configurations are obtained in office environment with line-

of-sight intra-office, non-line-of-sight corridor-office and corridor scenarios. Distances between transmitter and receiver up to 5 m for a frequency range from 2 GHz to 6 GHz have been used.

The small scale fading is extremely difficult to predict since it requires exact knowledge of the phase angle of each multipath component. For UWB channels, this phase is also frequency dependent. Fortunately, the fast fading (small scale fading) can be well characterised statistically. In this work, the UWB impulse response is the combination of antenna impulse response and the channel impulse response itself. As the only available information about antennas is the radiation gain over the different frequency sub-bands, assumptions about the phase components have to be made. The total phase component resulting from the antenna and the multipath components assumed to be uniformly random distributed. Using these assumptions, an averaged vector sum of the different multipath components can be assessed. An average power delay profile is therefore derived for the combined channel transfer function.

3 UWB Measurement Procedure

Radio propagation studies can be performed either in time domain or in frequency domain. Most investigations of channel measurements have been performed in time domain using channel sounding techniques. These sounding techniques provide usually only a real estimation of the channel impulse response in time domain. However, frequency domain provides a complex estimation. This study has been performed in frequency domain through a Vector Network Analyser. The measurement method consists in exciting the channel with frequency sweeps over a wide range of frequencies from 2 GHz to 6 GHz. The attenuation and the phase shift of each frequency component caused by the propagation medium are measured. Furthermore, the channel impulse response in time domain is derived through the inverse Fourier transform of the measured transfer function. During the measurements, the frequency band is swept from 2 GHz to 6 GHz (4 GHz of frequency span) with 801 points corresponding to a 5 MHz frequency step. Therefore, a multipath can be measured with a time delay up to 200 ns. Moreover, the time domain resolution corresponds to the ability to resolve two closely-spaced propagation paths. A minimum band pass impulse window (rectangular) leads to a response resolution of 0.3 ns, whereas a maximum band pass impulse window (e.g. Blackmann) leads to a response resolution of 0.57 ns. In this analysis, measurements have undergone a Hamming windowing.

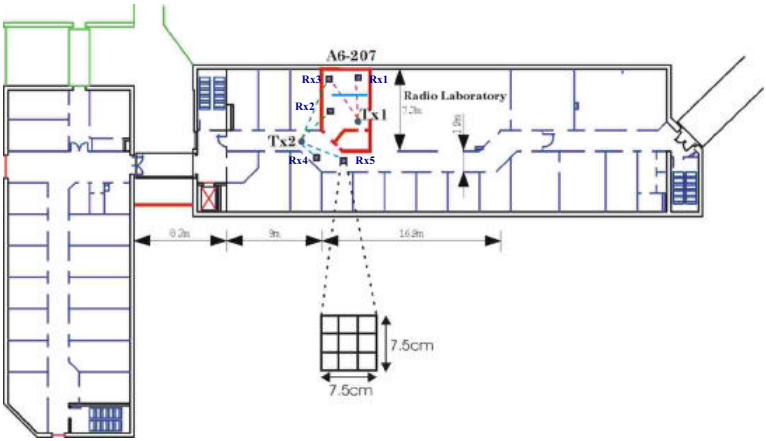

Figure 4. Measurement Locations

The measurements were conducted at the building of the Antenna and Propagation Division at Aalborg University as shown in Figure 4. The position Tx1 of the transmitter corresponds to LOS intra-office measurements, whereas the Tx2 position is for both LOS corridor and NLOS corridor-office measurements. Considering a Wide Sense Stationary Uncorrelated Scattering (WSSUS) indoor channel, impulse responses collected in the same area are very similar due to the channel invariance over short distances. Therefore, impulse responses are collected in nine locations within a grid of 7.5 cm x 7.5 cm, with a spacing of 2.5 cm corresponding to $\lambda/2$ at the highest frequency within the frequency sweep [8]. Note that in general the WSSUS assumption for indoor UWB channels is not fulfilled. Further investigations of the effect of this simplifying assumption are required.

4 Comparison of measurements with the prediction model

In this section, channel parameters obtained from measurements and derived from blind predictions will be compared for LOS office (Figure 5a and 5b), LOS corridor (Figure 5c and 5d) and NLOS corridor-office.

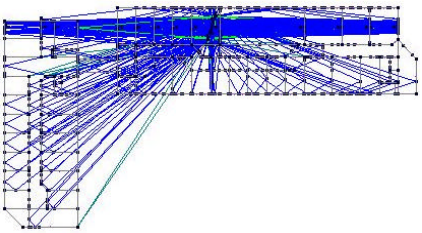

Figure 5a. 2D View of LOS simulation in the room A6-207 with up to 2nd reflection order

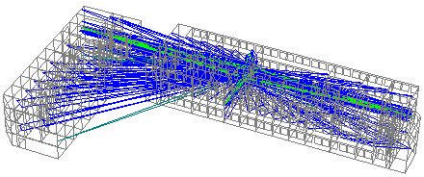

Figure 5b. 3D View of ray tracing simulation

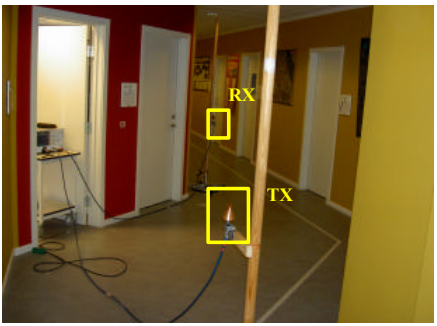

Figure 5c. Tx and Rx position on the floor

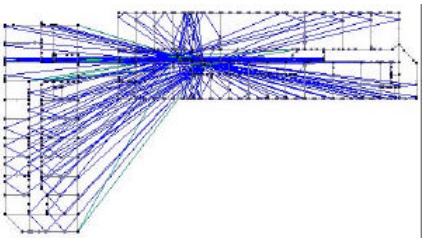

Figure 5d. 2D View of LOS simulation in the room A6-207 with up to 2nd reflection order

In order to improve the visibility of Figure 5a, 5b and 5d, only interactions up to the second order are plotted. For these configurations, large-scale parameters such as power decay factor and mean path loss at different frequencies will be compared. Moreover, RMS delay spread and the correlation factor are two parameters to be compared. The time dispersion properties of wide band multipath channels are most commonly quantified by the mean excess delay ($\bar{\tau}$) and the RMS delay spread (σ_τ), whereby both

parameters are the first moment and the square root of the second central moment of the power delay profile, respectively.

4.1 LOS Measurements: intra-office

The first measurements were conducted in LOS condition in the office A6-207 where the transmitter is Tx1 and the receiver is Rx1 as shown in Figure 4. The prediction with the sub-band ray tracing shows the frequency decay characteristic and the frequency selective fading of the channel (See Figure 6a). Both measured and predicted UWB channel transfer functions follow a similar power decay with frequency (Table 1). A faster decay is observed beginning from the central frequency 4 GHz. In time domain (See Figure 6b), the impulse response shows a small delay spread for both simulation and measurement. An extinction of the multipath is noticeable for larger delay times, therefore only the first 30 ns are presented to show two multipath clusters. However, the measurement also present an individual reflection at 22 ns which does not appear in the model.

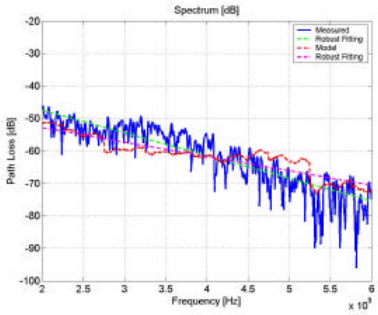

Figure 6a. Measured and simulated transfer function in frequency domain with a robust fitting of the power decay factor

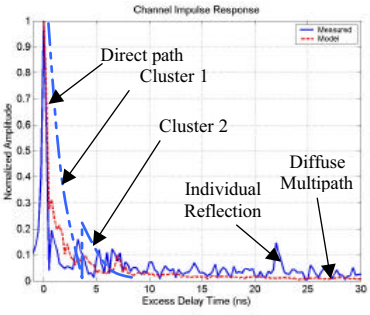

Figure 6b. Measured and simulated channel impulse response for LOS

The predicted spectrum envelope exhibits a general decay following the measurements. A robust linear regression fit has been performed for both prediction and measurements as shown in Figure 6a. The power decay factor for the measurements is similar to the one for the prediction (Tab. 1). In order to measure the degree of similarity of the measurement and the model a correlation coefficient is calculated. The correlation coefficient between the transfer function of the measurement and the transfer function of the model is 0.82.

The Saleh and Valenzuela indoor statistical model [9] assumes that the multipath components arrive in clusters. The amplitudes of the received components are independent Rayleigh random variables with variance that decays exponentially with cluster delay as well as with excess delay within a cluster. These multipath components within a cluster have exponentially distributed interarrival times [10]. Figure 6b shows a LOS impulse response according to the cluster model. Two clusters are noticeable. The main cluster containing the direct path with short reflections from the floor and the ceiling superposes for both measurements and simulations.

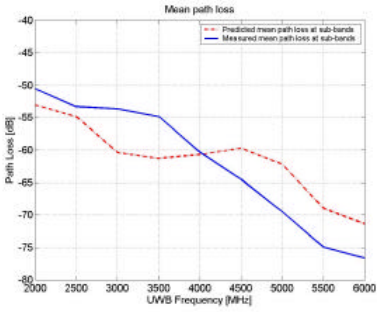

Figure 7a. Predicted path loss over the nine sub-bands

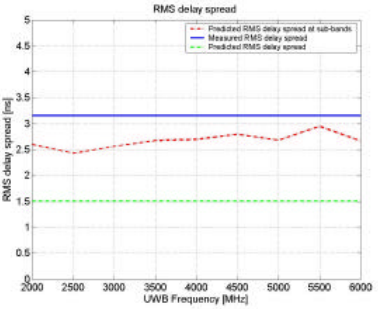

Figure 7b. Predicted and measured RMS delay spread over the sub-band

The predicted and measured path loss at each sub-band are comparable. Both measurement and model intercept at the central frequency 4 GHz. Prior to this frequency the path loss is underestimated and after this frequency the path loss is overestimated. A more detailed quantitative evaluation is given in Table 1. In Figure 7b the RMS delay spread is underestimated for all frequencies. That could be the result since the model has not yet been calibrated and since the model does not take into account scattering at higher frequencies.

4.2 LOS Measurements on the corridor

Measurements were conducted on the corridor where the transmitter Tx2 and the receiver Rx4 are 4.4 m away from each other, as shown in the layout of Figure 4 and the picture of Figure 5c. A 2D view of the 3D ray tracing propagation prediction corresponding to the LOS corridor measurements is presented in Figure 5d, where reflection up to the second order is considered. Measured and simulated transfer functions in frequency domain are presented in Figure 8a, where a difference is noticeable. In terms of large-scale parameters, the path loss undergoes a decay over increasing frequency. The power decay factor for the measurements is smaller than the one for the prediction. The measured decay factor exceeds the predicted one. A robust linear regression fit has been performed for both prediction and measurements as in Figure 8a.

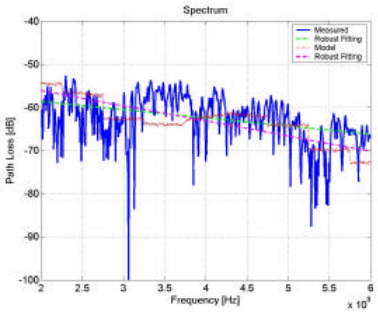

Figure 8a. Transfer function and power decay

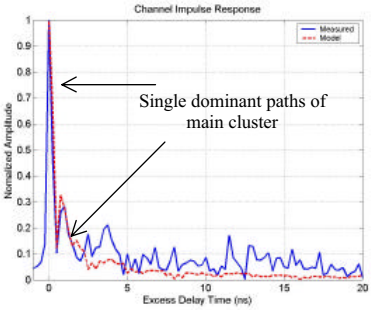

Figure 8b. Channel impulse response

Figure 8b presents the measured impulse response for LOS corridor with a focus on the time domain up to 20 ns in order to better identify dominant propagation paths. Under LOS conditions and for corridor measurements the received power envelope is Ricean distributed. A single dominant path within the main cluster is identified.

The high resolution enables the identification of certain main propagation paths mainly due to specular reflections. The deterministic model shows a main cluster with higher power propagation paths and a shorter delay spread of σ_{τ_Sim}=1.34 ns, whereas in the measurements the same cluster has lower power. Moreover, at a later time other propagation paths are noticeable as well, which leads to a little higher delay spread of σ_{τ_Meas}=5.1 ns. The amplitude difference between both measurements and prediction is due to the a priori material parameter values used for the blind prediction. A calibration could be performed in order to get a better fit to the measurements. More detailed results are found in Table 1.

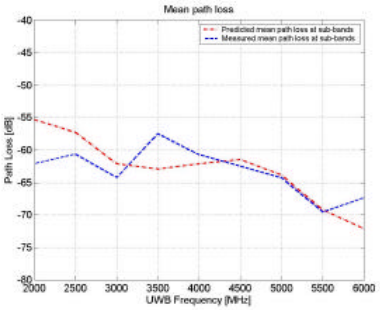

Figure 9a. Predicted path loss over the nine sub-bands

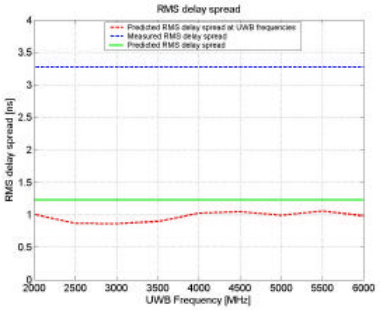

Figure 9b. Predicted RMS delay spread over the sub-bands

In terms of large scale parameters, the path loss is better predicted in the second half of the bandwidth where both the model and the measurement converge. The RMS remains, however, underestimated in this case.

4.3 NLOS Measurements for corridor-office

These measurements were conducted with a transmitter Tx2 on the corridor and the receiver Rx1 in the room A6-207 as shown in Figure 4. In this NLOS case it is obvious that other reflected propagation paths gain power over the direct path. In comparison to the LOS case for inter-office and for corridor as well, the channel impulse response shows certain small dominant paths directly after the direct path which also has been proved by the blind prediction. However, the corresponding amplitudes could be corrected through calibration procedures. Blind predictions show an RMS delay spread of σ_{τ_Sim}=1.6 ns, whereas the measured delay spread is σ_{τ_Meas}=12.3 ns. The difference might be due to the distribution of power on the different propagation paths. It can be stated that blind predictions still perform better in terms of time dispersion parameters in LOS cases for inter-office and corridor than in NLOS ones. Moreover an overall better performance is seen for large-scale parameters.

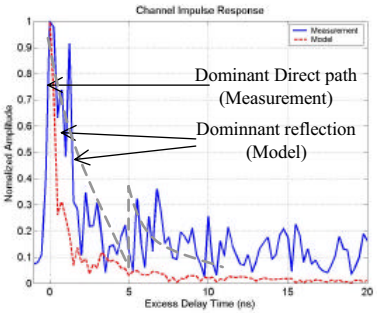

Figure 10a. Impulse response for NLOS corridor-office

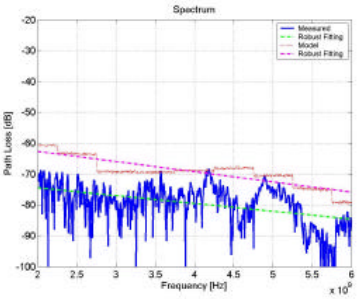

Figure 10b. Measured and simulated transfer function with a robust fitting of the power decay

Table 1 resumes the different results for measurements, where L is the path loss, α is the power decay factor and σ_τ is the RMS delay spread. The configuration Tx1-Rx2, Tx2-Rx4 and Tx2-Rx1 can be found in [11], where the authors presented a preliminary results of this investigation. In [11] no phase distribution over multipath components has been considered. Additionally, a rectangular windowing is applied to the impulse response. In the present work an averaging of power delay profiles has been considered using in the model a uniform randomly distributed phase over the multipath components. Furthermore, in order to better estimate the amplitude and time of arrival of multipath components a Hamming windowing has been applied.

	LOS Intra-Office						**LOS Corridor**				**NLOS Corridor-Office**			
	Tx1-Rx1		**Tx1-Rx2**		**Tx1-Rx3**		**Tx2-Rx4**		**Tx2-Rx5**		**Tx2-Rx2**		**Tx2-Rx1**	
	Meas	Mod	Meas	Mod	Meas	Mod	Meas	Mod	Meas	Mod	Meas	Mod	Meas	Mod
L(dB)	-58.6	-59.3	-53.2	-54	-56	-57.6	-55.9	-60.9	-57.9	-56.2	-66.2	-62.7	-70.5	-82.7
α(dB/MHz)	0.08	0.05	0.03	0.03	0.05	0.05	0.04	0.05	0.05	0.05	0.05	0.05	0.06	0.08
σ_τ (ns)	7.7	1.8	3.15	1.53	5.9	1.6	5.1	1.34	3.27	1.15	11.9	0.8	12.3	1.6

Table 1. Measurement and prediction results

In this work, a better model fit to the measurements is seen for large-scale parameters (path loss, power decay factor), especially in LOS conditions. Time dispersion parameters are also better predicted in LOS conditions than in the NLOS ones. However, these have still to be improved through the model calibration.

5 Conclusion

This work has focused on the applicability of deterministic modelling through 3D ray tracing blind prediction to ultra-wideband channels. The goal was to check performance of this modelling approach, based on the a priori knowledge of material parameters as well as on antenna power gain patterns, over the frequency sweep of use. Investigations by means of measurements as well as by means of blind predictions were performed in order to check the main characteristics of UWB channels: resolvability of propagation paths, frequency dependent power decay and frequency selective fading.

This study has shown that the blind prediction approach performs well in most cases in terms of large-scale parameters (e. g. total path loss). However, time dispersion parameters remain more sensitive to the frequency selectivity character of the UWB channel. A maximum deviation is registered in the NLOS case of corridor-office. In further work the calibration of the prediction model in terms of electromagnetic material parameters and also a comparison of the measurements with simple indoor empirical models [12] will be continued.

6 References

[1] Zuendt et al., Integration of Indoor Positioning into a Global Location Platform, WPNC'04 Proceeding, pp. 55-66.

[2] Andreas F. Molish, Ultra-Wideband propagation channels – theory, measurement, and modelling. Submitted to IEEE Transactions on Vehicular technology, winter 2005.

[3] Jürgen Kunisch and Jörg Pamp, "An Ultra-Wideband Space-Variant Multipath Indoor Radio Channel Model", *COST 273 TD (03) 154*.

[4] Hiroto Sughara, Yoshinori Watanabe, Takashi Ono, Kazuhiro Okanoue, and Shuntaro Yamazaki, " Development and Experimental Evaluations of "RS-2000" ~A Propagation Simulator for UWB Systems~", in *Proc. IEEE UWBST 04*, pp. 76–80, 2004.

[5] "Ultra-Wideband Propagation Measurements and Modelling Final Report", DARPA NETEX Program, Virginia Tech, January 31st, 2004.

[6] Hong C. Rhim and Oral Büyüköztürk, "Electromagnetic Properties of Concrete at Microwave Frequency Range", ACI Materials Journal, pp. 262-271, May-June 1998.

[7] Mohammad Firoz Kabir et. al, Temperature Dependence of the Dielectric Properties of Rubber Wood, Wood and Fiber Science, 33(2), 2001, pp. 233–238.

[8] J. Keignart and N. Daniele, "Subnanosecond UWB Channel Sounding in Frequency and Temporal Domain", *in Proc. IEEE Conf. Ultra Wideband Systems and Technologies*, 2002, pp. 25–30.

[9] A. Saleh and R. Valenzuela, "A statistical model for indoor multipath propagation," *IEEE J. Select. Areas Commun.*, vol. SAC-5, pp. 128–137, Feb. 1987.

[10] Theodore S. Rappaport, "Wireless Communications, Principles and practice", Second Edition, ISBN 0-13-042232-0.

[11] J. Jemai, Patrick C. F. Eggers, Gert Frølund Pedersen, "On the Applicability of Deterministic Modelling to Indoor UWB Channels", COST 273, TD(05)120.

[12] COST Action 231, Digital mobile radio towards future generation systems, Final Report, European Commission 1999